Fermi National Accelerator Laboratory

TM-1556

Coupled Transverse Motion*

Lee C. Teng
Fermi National Accelerator Laboratory
P.O. Box 500, Batavia, Illinois

January 1989

* Lecture given at Joint U.S.-CERN School on Particle Accelerators, Capri, Italy, October 20-26, 1988.

Operated by Universities Research Association Inc. under contract with the United States Department of Energy

COUPLED TRANSVERSE MOTION

Lee C. Teng
Fermi National Accelerator Laboratory
Batavia, Il. 60510

I. Introduction

The magnetic field in an accelerator or a storage ring is usually so designed that the horizontal (x) and the vertical (y) motions of an ion are uncoupled. However, because of imperfections in construction and alignment, some small coupling is unavoidable. In this lecture, we discuss in a general way what is known about the behaviors of coupled motions in two degrees-of-freedom.

II. General Features of Hamiltonian Dynamics

Since the single particle dynamics in a magnetic ring is Hamiltonian, some general behaviors are exhibited. The motion is Hamiltonian at all times. It is, therefore, equivalent to the unfolding of a continuous canonical transformation since by definition a canonical transformation preserves the Hamiltonian formalism. There are a number of expressions of local dynamical variables which are invariant under canonical transformations and, are therefore, local invariants of motion. The most useful is the Poisson bracket of any two dynamical variables F and G defined by

$$[F,G] = \sum_i \begin{vmatrix} \frac{\partial F}{\partial q_i} & \frac{\partial F}{\partial p_i} \\ \frac{\partial G}{\partial q_i} & \frac{\partial G}{\partial p_i} \end{vmatrix} = -[G,F] \tag{1}$$

Where q_i, p_i are the coordinate and conjugate momentum variables of the motion. Two interesting properties of the Poisson bracket are

$$[q_i,p_j] = \delta_{ij} \tag{2}$$

and

$$\dot{F} = [F,H] \tag{3}$$

where H is the Hamiltonian and dot means d/dt. The canonical equation of motion can thus be written as

$$\begin{cases} \dot{q}_i = [q_i, H] \\ \dot{p}_i = [p_i, H] \end{cases} \tag{4}$$

The Poisson bracket also provides the transition to quantum mechanics where it is replaced by the commutator, i.e.

$$[F,G] \rightarrow \frac{1}{i\hbar}(FG-GF) \tag{5}$$

Also interesting are the Poincaré integral invariants. For an n degree-of-freedom motion, the n integrals

$$\begin{cases} \int_{S_2} \sum_i (dq_i dp_i), \\ \int_{S_4} \sum_{i,j} (dq_i dp_i dq_j dp_j), \\ \cdots\cdots \\ \int_{S_{2n}} dq_1 dp_1 dq_2 dp_2 \cdots dq_n dp_n \end{cases} \tag{6}$$

are all invariants of motion. The integration domain S_{2m} ($m \leq n$) is an arbitrary 2m-dimensional manifold in the 2n-dimensional phase space. In our case of n=2 we have only two invariants. The first one

$$\int_{S_2} (dxdp_x + dydp_y) = \text{proj. of } S_2 \text{ on } (x, p_x) \text{ plane} + \text{proj. of } S_2 \text{ on } (y, p_y) \text{ plane} = \text{invariant} \tag{7}$$

is not very useful, because we are normally interested in the projections of a 4-dimensional phase space volume (projected x and y emittances) and not those of S_2. We shall see below that under certain special cases, one can indeed make some statements about the projected x and y emittances for a coupled motion. But the relations are by no means simple. The second

$$\int_{S_4} dxdp_x dydp_y = \text{4-dimentional emittance} = \text{invariant} \tag{8}$$

is the Liouville theorem and is, of course, most useful.

III. Coupled Linear Motion

A. Parametrization

A general quadratic Hamiltonian can always be transformed to the following form

$$H = \frac{1}{2}(p_x^2 + p_y^2) + L(yp_x - xp_y) + \frac{1}{2}K_x x^2 + Qxy + \frac{1}{2}K_y y^2$$

$$= \frac{1}{2}\begin{pmatrix} x & p_x & y & p_y \end{pmatrix} \left(\begin{array}{cc|cc} K_x & 0 & Q & -L \\ 0 & 1 & L & 0 \\ \hline Q & L & K_y & 0 \\ -L & 0 & 0 & 1 \end{array}\right) \begin{pmatrix} x \\ p_x \\ y \\ p_y \end{pmatrix} \equiv \frac{1}{2}\tilde{Z}HZ \tag{9}$$

where the L (angular momentum) and the Q (45° roll) coupling terms are due respectively to solenoids and skew quadrupoles. The twiddle means transposition and the cross in a 4x4 matrix divides it into four 2x2 matrices. The corresponding canonical equations of motion can be written as

$$\dot{Z} = SHZ \tag{10}$$

with

$$S \equiv \left(\begin{array}{cc|cc} 0 & 1 & & \\ -1 & 0 & \multicolumn{2}{c}{0} \\ \hline & & 0 & 1 \\ \multicolumn{2}{c|}{0} & -1 & 0 \end{array}\right) = \text{symplectic unit matix}$$

The symplectic conjugate of a matrix M is defined as

$$M^+ \equiv S\tilde{M}\tilde{S} \tag{11}$$

A matrix is symplectic if $MM^+ = I$ or equivalently if $MS\tilde{M} = S$. The number of independent elements in a 2nx2n symplectic matrix is $s = n(2n+1)$.

For n=1 (one degree-of-freedom), s=3 and a 2x2 symplectic transfer matrix is parametrized by Courant and Snyder as

$$M = I\cos\mu + J\sin\mu \quad \text{with} \quad J = \begin{pmatrix} \alpha & \beta \\ -\gamma & -\alpha \end{pmatrix} \tag{12}$$

For n=2, s=10 and a 4x4 symplectic transfer matrix can be parametrized as[1]

$$T = \left(\begin{array}{c|c} M & m \\ \hline n & N \end{array}\right) = U\left(\begin{array}{c|c} A & 0 \\ \hline 0 & B \end{array}\right)U^{+} \tag{13}$$

where

$$U = \left(\begin{array}{c|c} I\cos\phi & D\sin\phi \\ \hline -D^{+}\sin\phi & I\cos\phi \end{array}\right)$$

and the 2x2 matrices A, B and D are all symplectic. Including ϕ this gives a total of 10 parameters for T. For the off-diagonal coupling terms, ϕ measures the strength and D gives the structure of the coupling. Some of the important relations are

$$D = \frac{m+n^{+}}{\Delta} \quad \text{with} \quad \Delta \equiv \sqrt{\det(m+n^{+})} = \text{real} \quad \text{near } \mu_x=\mu_y \tag{14}$$

$$\tan 2\phi = \frac{\Delta}{\mathrm{Tr}(M-N)/2} \tag{15}$$

$$A = M - Dn\tan\phi \tag{16}$$

$$B = N + D^{+}m\tan\phi \tag{17}$$

From these we get the Pythagoras relation

$$\left(\tfrac{1}{2}\mathrm{Tr}A - \tfrac{1}{2}\mathrm{Tr}B\right)^2 = \left(\tfrac{1}{2}\mathrm{Tr}M - \tfrac{1}{2}\mathrm{Tr}N\right)^2 + \Delta^2 \tag{18}$$

or

$$(\cos\mu_1 - \cos\mu_2)^2 = (\cos\mu_x - \cos\mu_y)^2 + \Delta^2 \ . \tag{19}$$

Thus the separation between the normal-mode phases μ_1 and μ_2 are always greater than that between the nominal horizontal and vertical phases μ_x and μ_y. The stronger is the coupling (the larger is ϕ) the greater is the separation between the normal-mode phases.

B. Invariants, Distributions and Emittances

From Eq. (13) one can immediately write two invariants W_1 and W_2 corresponding to the matrices A and B, each being a bilinear expression in all 4 phase-space variables x, p_x, y, p_y. When the motion is uncoupled (ϕ=0), the invariants are separated in the two degrees-of-freedom, such that

$$W_1 = W_x = \gamma_x x^2 + 2\alpha_x x p_x + \beta_x p_x^2 , \qquad W_2 = W_y \tag{20}$$

For one degree-of-freedom, the invariant distribution $\Psi(W)$ is elliptical. One can define a beam-ellipse matrix σ as in the computer program TRANSPORT[2]. As the motion progresses with transfer matrix M, the beam ellipse transforms like

$$\sigma = M \, \sigma_o \tilde{M} \tag{21}$$

and the emittance of the beam defined as the area of the ellipse is invariant.

For two degrees-of-freedom, the 2-dimensional manifold defined by a pair of values W_1 and W_2 is a torus. In general, then, the invariant distribution $\Psi(W_1, W_2)$ is rather complex. But if one takes only values of W_1 and W_2 such that $W_1+W_2=W$, one gets a one-parameter distribution which depends only on the sum of the "actions" in the two normal modes and which is, then, ellipsoidal. Although it is not clear how such an ellipsoidal beam may be formed, its behavior has many interesting features[3]. The beam-ellipsoid matrix is written in the TRANSPORT code as

$$\sigma = \left[\begin{array}{c|c} \sigma_x & t \\ \hline \tilde{t} & \sigma_y \end{array}\right] \tag{22}$$

and transforms with the transfer matrix T as

$$\sigma = T \, \sigma_o \tilde{T} \tag{23}$$

The x and y emittances ϵ_x and ϵ_y are defined as the areas of the projected ellipses. The following two relations for the projected emittances can be readily derived. In both cases, one starts with uncoupled emittances having upright ellipses in both planes (beam-ellipsoid matrix diagonal and denoted by subscript o).

Relation 1

$$\epsilon_x^2 - \epsilon_y^2 = (\epsilon_{xo}^2 - \epsilon_{yo}^2)(1 - 2\delta) , \qquad \delta \equiv \det(n) \tag{24}$$

where δ is the determinant of the lower-left coupling 2x2 matrix n of the transfer matrix T as given in Eq. (13). The obvious consequences of this relation are

(1) $\epsilon_x = \epsilon_y$ whenever $\delta = 1/2$.

and

(2) if $\epsilon_{xo} = \epsilon_{yo}$ then $\epsilon_x = \epsilon_y$ always.

Relation 2

$$\begin{cases} \epsilon_x \geq \epsilon_{xo} |1-\delta| + \epsilon_{yo} |\delta| \\ \epsilon_y \geq \epsilon_{xo} |\delta| + \epsilon_{yo} |1-\delta| \end{cases} \tag{25}$$

The consequences of these inequalities are:

(1) If $\epsilon_{yo} = 0$ and $\epsilon_{xo} \neq 0$, then

$$\begin{cases} \epsilon_x = \epsilon_{xo} |1-\delta| \\ \epsilon_y = \epsilon_{xo} |\delta| \end{cases}$$

and we have:

For $0 \leq \delta \leq 1$, $\epsilon_x + \epsilon_y = \epsilon_{xo}$; both ϵ_x and ϵ_y are bounded.

For $\delta > 1$ or $\delta < 0$, $|\epsilon_x - \epsilon_y| = \epsilon_{xo}$; ϵ_x and ϵ_y may be unbounded.

The situation is clearly symmetric if $\epsilon_{xo} = 0$ and $\epsilon_{yo} \neq 0$.

(2) If $\epsilon_{xo} = \epsilon_{yo} = \epsilon_o$, we have:

For $0 \leq \delta \leq 1$, $\epsilon_x = \epsilon_y \equiv \epsilon \geq \epsilon_o$. The growth of the projected emittance from ϵ_o to ϵ is not too large.

For $\delta > 1$ or $\delta < 0$, $\epsilon \geq \epsilon_o |2\delta-1|$. Depending on the value of δ the growth can be very large.

C. Decoupling Using Solenoids and Skew Quadrupoles[4].

The transfer matrix of a thin element has the form

$$T = \left(\begin{array}{c|c} I & F \\ \hline -F^+ & I \end{array}\right) \tag{26}$$

where for skew quadrupoles

$$F = k \begin{pmatrix} 0 & 0 \\ 1 & 0 \end{pmatrix} \quad \text{with} \quad k = \frac{B\ell}{B\rho} \tag{27}$$

and for solenoids

$$F = \theta \begin{pmatrix} 1 & 0 \\ 0 & 1 \end{pmatrix} \quad \text{with} \quad \theta = \frac{1}{2} \frac{B_z \ell}{B\rho} \ . \tag{28}$$

The quantities defining k and θ have their conventional meanings.

(1) For local compensation, we assume a number of thin coupling elements grouped closely together in a short section of the circumference of an otherwise linear and uncoupled ring. The condition that they produce zero coupling everywhere outside the short section is, to first order terms in the strengths of these elements

$$\Sigma\ M_x^{-1} F\ M_y = 0 \tag{29}$$

where

$$M_{x,y} = \text{uncoupled x or y transfer matrices from some fixed outside location to the element F}$$

and the summation is over all the coupling elements. Without writing them out explicitly, we see that this yields 4 conditions. Hence it takes, for example, 4 skew quadrupoles to compensate for the coupling produced, say, by the momentum analyzing solenoid in a colliding beams detector.

(2) To decouple the motions over a full revolution of the ring, all we need is to make Δ as defined in Eq. (14), vanish. For thin elements and to the first order, one can show that

$$\Delta^2 = -\ \mathrm{Tr} \sum_{ij} [M_x(ji) F_i M_y(ij) F_j^+ - \bar{M}_x(ji) F_i \bar{M}_y(ij) F_j^+] \tag{30}$$

Where F_i and F_j are as defined in Eqs. (27) and (28). $M_x(ji)$, e.g., is the uncoupled 2x2 transfer matrix in the x degree-of-freedom from location i to location j, and $\bar{M}_x(ji)$ is the same matrix but with $2\pi\nu_x$ added to the phase. To further clarify the notation of Eq. (30) we have for a single skew quadrupole

$$\Delta^2 = k^2 \beta_x \beta_y \sin 2\pi\nu_x \sin 2\pi\nu_y \quad . \tag{31}$$

The condition $\Delta = 0$ over a full revolution of the ring can clearly be satisfied with a single compensating skew quadrupole or in the case of a large ring, with a single string of skew quadrupoles all connected in series.

D. A Simplified Case

An overly simplified case which although unrealistic, is nevertheless illuminating is given by the Hamiltonian Eq. (9) with L = 0 (no solenoid) and

$$K_x \equiv \nu_x^2 \omega^2, \qquad K_y \equiv \nu_y^2 \omega^2, \qquad Q \equiv C \omega^2 \qquad \text{all constant,}$$

where ω = revolution angular frequency. The coupled equations of motion are now

$$\begin{cases} x'' + \nu_x^2 x + C y = 0 \\ y'' + \nu_y^2 y + C x = 0 \end{cases} \qquad \text{prime} = \frac{d}{d\theta} \tag{32}$$

The normal modes and frequencies are easily obtained by diagonalizing the matrix

$$\begin{pmatrix} \nu_x^2 & C \\ C & \nu_y^2 \end{pmatrix}$$

The normal coordinates are simply rotated from (x, y) by the angle Φ and the normal frequencies are

$$\begin{cases} \nu_1^2 = \nu_x^2 + C \tan \Phi \\ \nu_2^2 = \nu_y^2 - C \tan \Phi \end{cases} \tag{33}$$

with Φ defined by

$$\tan 2\Phi = \frac{2C}{\nu_x^2 - \nu_y^2} \tag{34}$$

The x and y motions with initial conditions x = 1, y = x' = y' = 0 at $\theta = 0$ are

$$\begin{cases} x = \cos^2 \Phi \cos \nu_1 \theta + \sin^2 \Phi \cos \nu_2 \theta \\ y = \sin \Phi \cos \Phi \, (\cos \nu_1 \theta - \cos \nu_2 \theta) \end{cases} \tag{35}$$

Both normal frequencies appear on both x and y motions (hence, beam pickups). It is, however, possible to rotate both the pickups and the beam kickers to the normal mode planes (angle Φ) to observe only ν_1 or ν_2. For $\nu_1 \doteq \nu_2$ the motions look like sinusoidally amplitude-modulated oscillations with angular frequency $(\nu_1 + \nu_2)/2$. The y-amplitude is zero at $\theta = 0$, grows to a maximum of

$$|y|_{max} = \sin 2\Phi \qquad (\text{and } |x| = |x|_{min} = \cos 2\Phi) \tag{36}$$

at $\theta = \pi/(\nu_1 - \nu_2)$ and returns to zero at $\theta = 2\pi/(\nu_1 - \nu_2)$. Thus a fraction $\sin 2\Phi$ of the amplitude (or a fraction $\sin^2 2\Phi$ of the energy) is coupled to swing back and forth between x and y.

IV. Coupled Non-linear Motion

Generally non-linear motions are not integrable and have to be treated either by the successive perturbation method or by a serial transformation procedure. The Hamiltonian is written as

$$H = H_o + H_1 \ . \tag{37}$$

The unperturbed Hamiltonian H_o contains only the uncoupled linear motions.

$$\begin{aligned} H_o &= \tfrac{1}{2}\,(p_x^2 + K_x x^2) + \tfrac{1}{2}\,(p_y^2 + K_y y^2) \\ &= \frac{R}{2\beta_x}\,(p_u^2 + u^2) + \frac{R}{2\beta_y}\,(p_v^2 + v^2) \\ &= 0 \qquad\qquad (2\pi R = \text{circumference}) \end{aligned} \tag{38}$$

where the second and the third expressions are those obtained after transformation first to the Floquet variables u, p_u, v, p_v (and $\theta = s/R$ as independent variable) by the generating function

$$F = -(\sqrt{\beta_x}\ u p_x + \frac{\alpha_x}{2}\ u^2) - (\sqrt{\beta_y}\ v p_y + \frac{\alpha_y}{2}\ v^2) \tag{39}$$

which gives

$$\begin{cases} x = \sqrt{\beta_x}\ u \\ p_x = \dfrac{1}{\sqrt{\beta_x}}(p_u - \alpha_x u) \end{cases} \qquad (\text{similarly for y}) \tag{40}$$

and second, to the angle-action variables a_x, I_x, a_y, I_y by the generating function

$$G = \frac{1}{2} p_u^2 \cot(\psi_x + a_x) + \frac{1}{2} p_v^2 \cot(\psi_y + a_y) \tag{41}$$

which gives

$$\begin{cases} u = \sqrt{2I_x} \cos(\psi_x + a_x) \\ \\ p_u = -\sqrt{2I_x} \sin(\psi_x + a_x) \end{cases} \qquad \text{(similarly for v)} \tag{42}$$

where

$$\psi_x \equiv \int \frac{ds}{\beta_x} = \text{linear betatron phase} \qquad \text{(similarly for y).}$$

In terms of the angle-action variables, the unperturbed Hamiltonian is zero indicating that in the angle-action phase space, the unperturbed motion is just a fixed point.

The perturbation Hamiltonian, H_1, is usually written in the multipole-expanded form. The 2k-pole term e.g. is

H_1(2k-pole term)

$$= \frac{1}{n!} \frac{B_y^{(k-1)}}{B\rho} \sum_m (-1)^{\frac{m}{2}} C_m^k x^{k-m} y^m \qquad \text{even m (normal)}$$

$$+ \frac{1}{n!} \frac{B_x^{(k-1)}}{B\rho} \sum_m (-1)^{\frac{m-1}{2}} C_m^k x^{k-m} y^m \qquad \text{odd m (skew)}$$

$$= \frac{1}{n!} \frac{B_y^{(k-1)}}{B\rho} \sum_m (-1)^{\frac{m}{2}} C_m^k (2\beta_x I_x)^{\frac{k-m}{2}} (2\beta_y I_y)^{\frac{m}{2}} \cos^{k-m}\phi_x \cos^m \phi_y$$

$$+ \text{ skew terms} \tag{43}$$

where

$\phi_{x,y} \equiv \psi_{x,y} + a_{x,y}$, C_m^k are the binomial coefficients,

and superscript (k-1) means $(k-1)^{th}$ derivative with respect to x. There are usually two interesting special simplifying approaches from this point on.

A. Single Resonance Dominated Motion.

If one expands the powers of cos ϕ, Fourier analyzes the θ-dependent coefficient into $\exp[\pm i(n\theta+\delta)]$ and finally substituting the index ℓ for (k-m), one gets for a single set of integral values of ℓ, m and n

$$H_1(\ell\nu_x + m\nu_y = n \text{ resonant term}) = K_{\ell mn}(2I_x)^{\frac{\ell}{2}} (2I_y)^{\frac{m}{2}} \cos \phi_{\ell mn} \tag{44}$$

with

$$\phi_{\ell mn} = (\ell\psi_x + m\psi_y - n\theta) + \ell a_x + m a_y - \delta$$

$$\tilde{=} (\ell\nu_x + m\nu_y - n)\theta + \ell a_x + m a_y - \delta$$

The single resonance dominated motions have been studied extensively[5, 6, 7, 8]. Their general features of fixed points, separatrices, etc., are familiar to most people and will not be further pursued here. We will only point out that for resonances in a single plane an important application is the resonant beam extraction and that for coupled resonances the Hamiltonian, Eq. (44), yields readily the invariant

$$mI_x - \ell I_y = \text{invariant} \tag{45}$$

which states that on a difference resonance (ℓ and m have opposite signs) the motion is bounded.

B. Away From Resonances

Since resonances are everywhere dense as rational numbers, we can only mean here that the motion is away from strong low-order resonances. In this case, the effects of the low-order resonances are to distort the unperturbed linear motion. The distortions are given in terms of the distortion functions[9] which are most conveniently defined in the complex form. The unperturbed motions are written as

$$z_x \equiv u + ip_u = \sqrt{2I_x}\, e^{-i\phi_x} \qquad \text{(same for y)} \tag{46}$$

For a given 2n-pole perturbation term the distortions δz_x and δz_y are given as polynomials in z_x, z_x^*, z_y, z_y^* of the $(n-1)^{th}$ degree. The coefficients of the polynomial terms denoted by the letter D are the distortion functions. They can be derived either by solving the perturbed orbit equations of motion to the lowest order approximation using the method of Variation of Parameters or by applying the standard lowest order perturbation treatment on the perturbed Hamiltonian[10]. For a normal sextupole perturbation term for example, we have

$$\begin{cases} \delta z_x = D_1^* z_x^2 - D_3 z_x^{*2} + D_+ z_y^{*2} - D_-^* z_y^2 \\ \delta z_y = 2(-D^* z_x z_y + D z_x^* z_y + D_- z_x z_y^* + D_+ z_x^* z_y^*) \end{cases} \tag{47}$$

The quadratic dependencies of δz_x and δz_y on z_x and z_y are those expected to arise from a sextupole term. The D's are the distortion functions having the form D=B+iB' (prime means differentiation with respect to the argument) and the B's have the following characteristics:

(1) Each has an appropriate resonant denominator, e.g.,

$$B_3 \propto \frac{1}{\sin 3\pi\nu_x}, \quad B_\pm \propto \frac{1}{\sin \pi(2\nu_y \pm \nu_x)}, \qquad \text{etc.} \tag{48}$$

Thus, the distortion functions blow up when exactly on resonance.

(2) The numerators are summations of the "strengths" of the sextupoles (assumed thin) properly scaled by the β-functions and multiplied by the appropriate linear phase factors at their individual locations.

One can, in addition, express the closed orbit distortions and the betatron tune shifts in terms of these distortion functions. The exact expressions of the distortion functions up to the octupole perturbation term are given in Ref. 10.

Figs. 1 and 2 show mappings of the motion with a random distribution of sextupoles obtained by particle tracking. Fig. 1 shows the typical scatter of projections of the phases points on the (u, p_u) and the (v, p_v) planes. In Fig. 2, the distortions of the motion as computed by Eq. (47) have been subtracted from the plot in Fig. 1. This results in the nearly perfect linear betatron motions as represented by the circles, showing that Eq. (47) gives the distortions due to the sextupoles to very good approximations.

C. All Non-linearity Included.

Either away from resonances or single resonance dominated the motion is regular and as seen above, is pretty well understood and predictable. But when all non-linearities and resonances are included, the well known stochastic regime of motion (chaos) appears together with such phenomena as stochastic layers, bifurcations, Arnol'd diffusion, overlapping of resonances, etc. Non-linear dynamics has been the subject of concentration of many prominent mathematicians such as Poincarē, Birkhoff, Kolmogorov, Arnol'd, Moser, Chirikov, Feigenbaum, etc. The relevance of these interesting non-linear phenomena to accelerator technology is so far limited to determining the domain of the stochastic regime and avoiding it.

The most reliable and productive approach to the study of non-linear dynamics has so far been by numerical simulation. Many computer programs have been written. They

generally fall into two distinct categories. For particle tracking one uses the "kick codes" in which the non-linear effects are represented by frequent and regular non-linear kicks. Programs of the second category integrate the non-linear motion by successive approximations using the Moser transformation[5] or the Lie algebra[11] techniques.

V. Measurements

We give here a very brief discussion of the principles of beam sensors and the general features of measurements.

A. Beam Sensors

We list here only transverse non-destructive induction sensors. They are classified by the type of induction used to derive the signal:

Electric (charge), Magnetic (current) or Electromagnetic.

They can also be classified by the moment of the transverse beam distribution or motion to be measured:

Monopole (beam current), Dipole (beam position), Quadrupole (beam ellipticity), etc.

We shall illustrate the different induction types by a beam position (dipole) monitor.

(1) Electric pickup monitor: The original form is the split electrode shown in Fig. 3. The beam coupling impedance Z/n of such a structure is rather high leading to a low threshold for coherent beam instability. The most commonly used structure now is shown in Fig. 4. The electrodes are reduced to the size of large buttons and are mounted flush with the vacuum chamber to reduce the coupling impedance. The typical sensitivity of this type of position monitor is around 100 μm.

(2) Magnetic pickup monitor: The original form starts with a ferrite ring to pick up high frequency magnetic inductions (Fig. 5). The signals are the currents picked up by the four coils used as two diametrically opposite pairs, one each for horizontal and vertical positions. This type of monitor has a low sensitivity and a high coupling impedance and is, therefore, seldom used in a ring accelerator. But it has certain advantages when used on a single-pass transport beam. It is especially useful as a beam current monitor (monopole sensor) with all four coils connected in series. Indeed all position monitors can be used as beam current monitors simply by taking the sum of the signals from all the electrodes.

(3) Electromagnetic pickup monitor: This is also known as the stripline monitor. A long narrow electrode placed lengthwise next to the vacuum chamber forms a parallel-plate stripline (Fig. 6). The geometry is usually chosen to yield a 50Ω impedance. The ends of the electrodes are led out of the vacuum pipe by feed-through insulators. If one end is terminated and the signal at the other end is read through a 50Ω cable, we have a directional sensor. The highest sensitivity is obtained when the stripline is a quarter wavelength long and can be better than 50μm. Depending on the geometry, the beam coupling impedance of the stripline monitor can be made rather modest.

Any combined horizontal-vertical position monitor can be used as an "ellipticity" quadrupole moment monitor by taking the difference of the sum-signal of the horizontal pair and that of the vertical pair. Extrapolating in this manner, one can in principle construct monitors for higher moments. However, the sensitivity of these monitors drop rather sharply for higher order moments.

B. General features of measurements

We make here a few simple but important observations and remarks about beam measurements.

(1) The signals can be presented either in the time-domain or through an FFT, in the frequency-domain.

(2) In a synchroton during acceleration, only adiabatically varying quantities can be presented in the f-domain with any reasonable accuracy.

(3) In storage rings with schottky measurements, the measurement time can be made extremely long. Thus, one can obtain very high precisions for measurements in the f-domain. This is the reason that an accurate tune-plot is easy to obtain for a storage ring.

(4) To measure a coherent motion, one needs to kick the beam. Such a measurement is difficult because first, one measures only the average motion of a rather large and diffuse beam and second, the decoherence time of the large beam is rather short. Thus, coherent measurements generally have rather poor accuracy in either t- or f-domain. Hence, accurate phase-plots are difficult to obtain.

(5) The measurement of an electron beam is made much easier by the availability of the synchrotron radiation which gives a faithful representation of the beam.

REFERENCES

1. D.A. Edwards and L.C. Teng, IEEE Trans. Nucl. Sci., Vol NS-20, No. 3, p.885 (1973).

2. K.L. Brown, D.C. Carey, Ch. Iselin and F. Rothacker, TRANSPORT, A Computer Program for Designing Charged Particle Beam Transport Systems, SLAC 91 (1973 rev.), NAL 91, and CERN 80-04.

3. K.L. Brown and R.V. Servranckx, "Cross Plane Coupling and the SLC Arcs" - to be published in Part. Acc.

4. S. Peggs, IEEE Trans. Nucl. Sci. Vol. NS-30, No. 4, p. 2460 (1983).

5. J. Moser, Nach. Akad. Wiss. Gottingen, IIA, No. 6, 87 (1955).

6. A. Schoch, CERN Report, CERN 57-23 (1958).

7. P.A. Sturrock, Ann. Phys. 3, 113 (1958).

8. W.P. Lysenko, Part. Acc. 5, 1 (1973).

9. T.L. Collins, Fermilab Report, Fermilab 84/114 (1984).

10. N. Merminga and K.-Y. Ng, "Hamiltonian Approach to Distortion Functions", Fermilab Report FN-493 (1988).

11. A.J. Dragt, F. Neri, G. Rangarajan, D.R. Douglas, L.M. Healy, and R.D. Ryne, Ann. Rev. Nucl. Part. Sci. 38, 455-496 (1988).

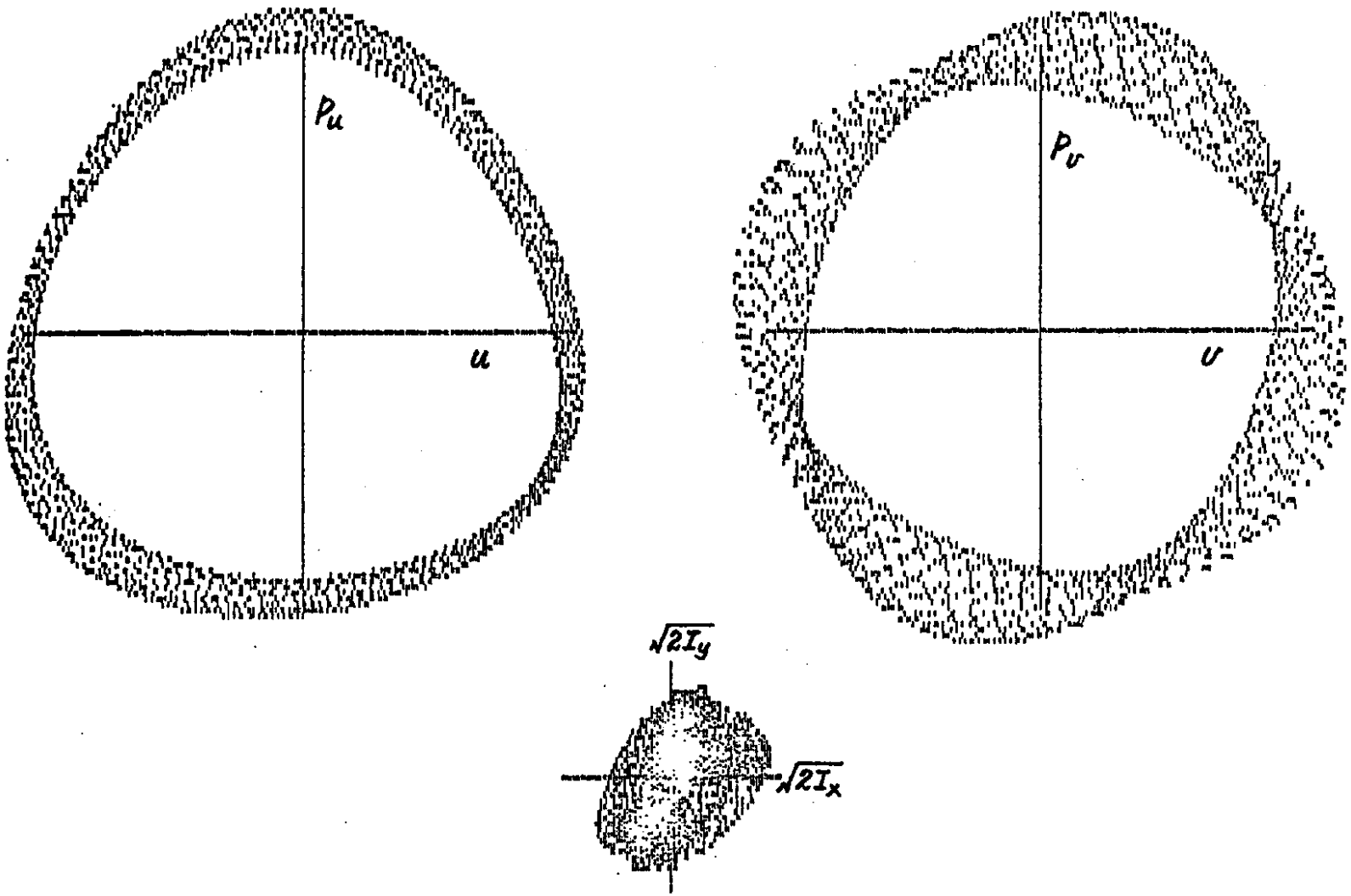

Fig. 1 Mapping of the motion with a random distribution of sextupoles obtained by particle tracking. This shows the typical scatter of projections of the phase points on the (u, p_u) and the (v, p_v) planes.

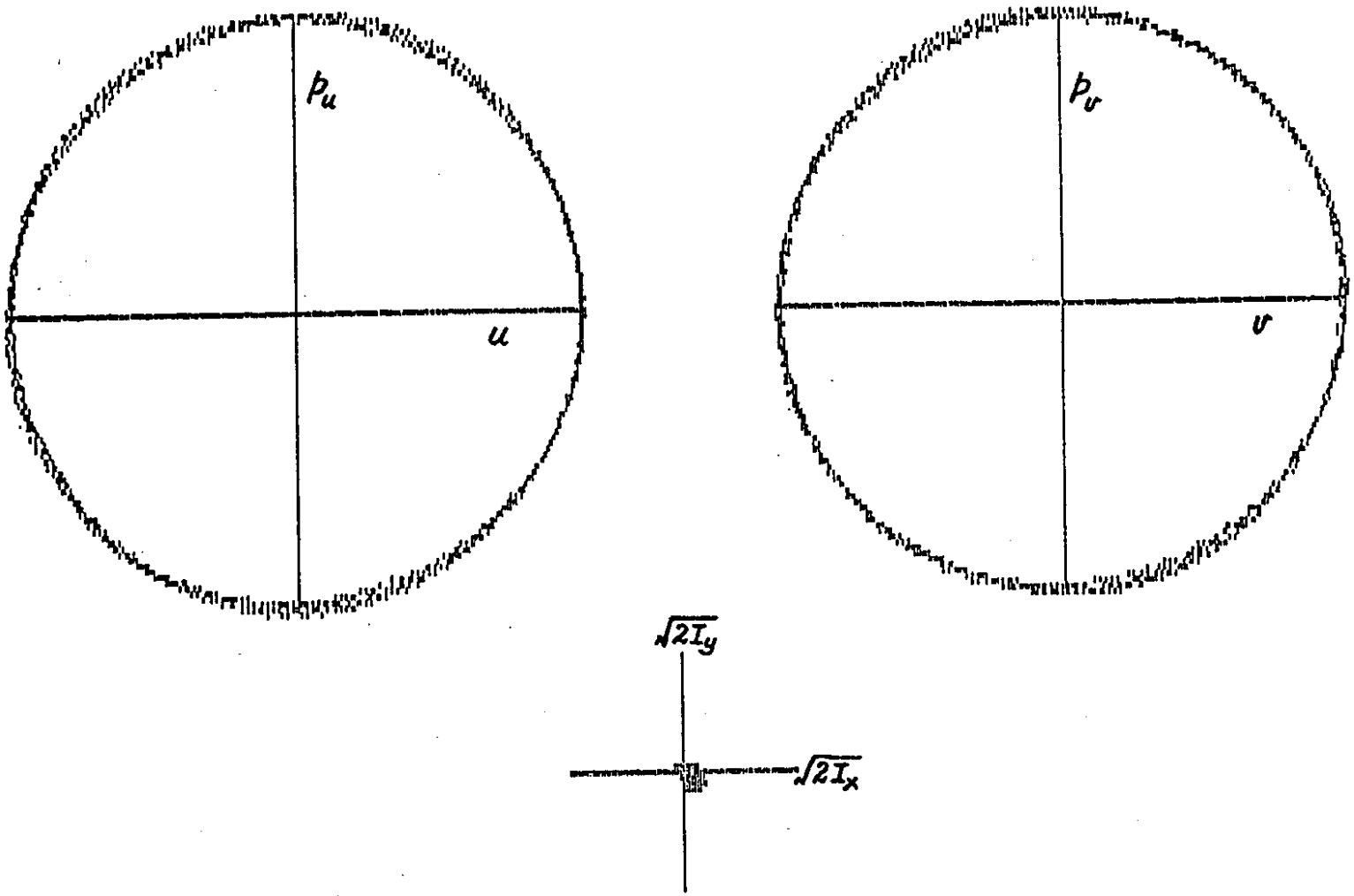

Fig. 2 Same mapping as in figure 1 but with the sextupole distortions given by the distortion functions subtracted from the tracking results. The resulting nearly perfect linear motion shows that the distortion functions give very good approximations.

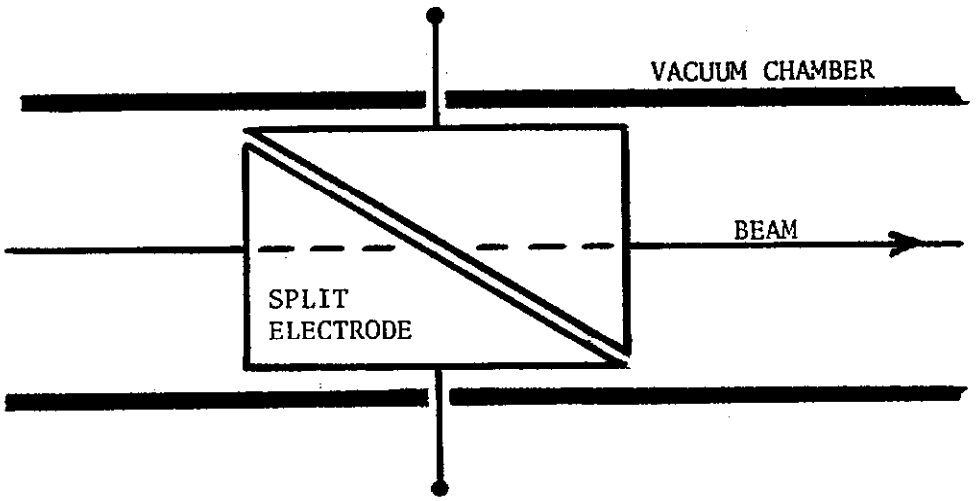

Fig. 3 Schematic top-view of a pair of split electrodes for a beam position monitor.

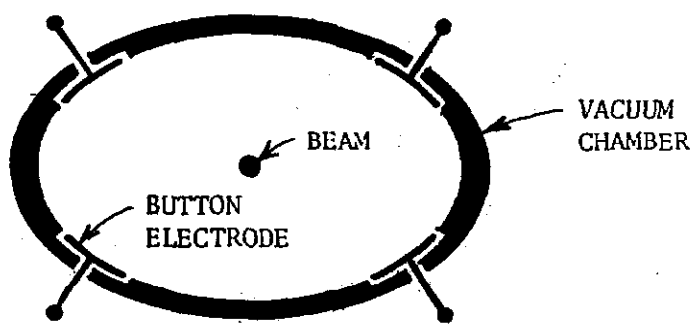

Fig. 4 Schematic end-view of the "button" electrodes for a beam position monitor.

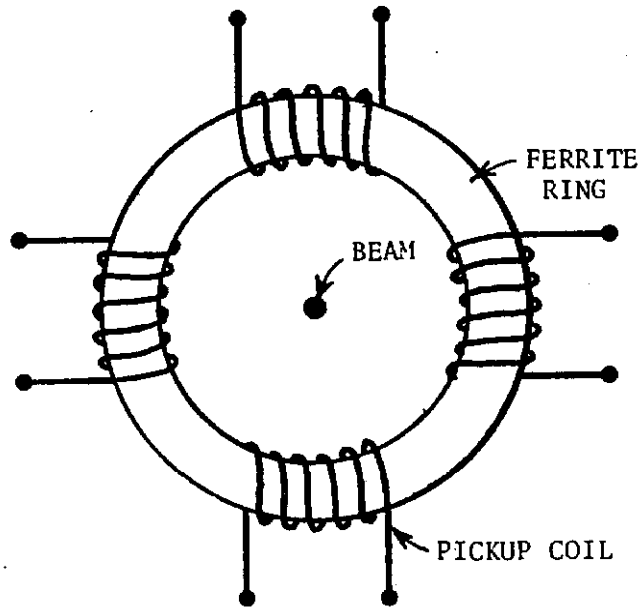

Fig. 5 Schematic end-view of a ferrite-ring magnetic pickup beam position monitor.

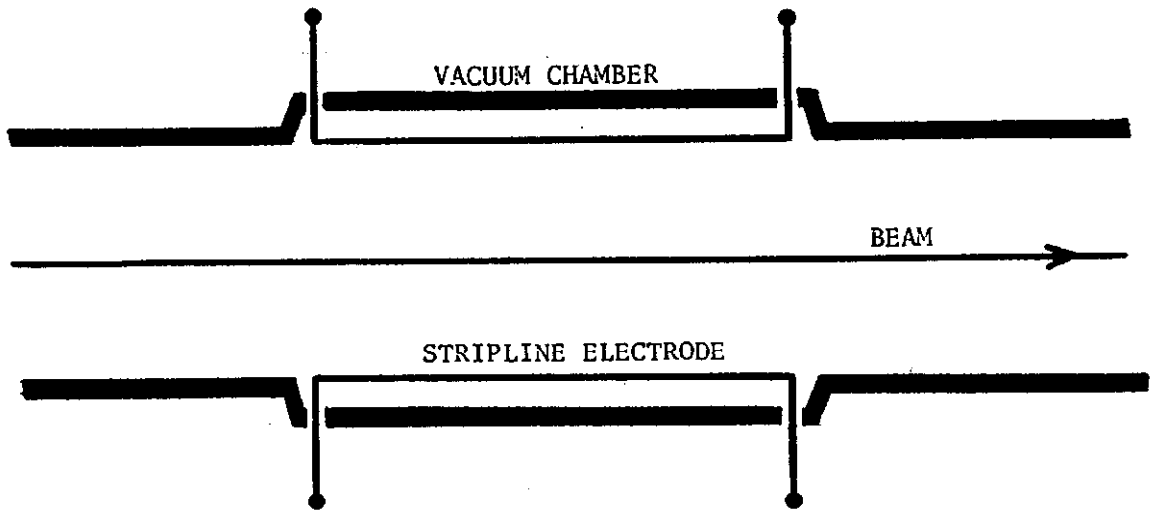

Fig. 6 Schematic side-view of a pair of stripline electrodes for a stripline beam monitor.